Setup for microwave stimulation of a turbulent low-swirl flame

Ehn, Andreas; Hurtig, Tomas; Petersson, Per; Zhu, Jiajian; Larsson, Anders; Fureby, Christer; Larfeldt, Jenny; Li, Zhongshan; Aldén, Marcus

Published in:
Journal of Physics D: Applied Physics

DOI:
10.1088/0022-3727/49/18/185601

2016

Document Version:
Peer reviewed version (aka post-print)

This is the peer reviewed version of the following article: [1], which has been published in final form at https://doi.org/10.1088/0022-3727/49/18/185601

[1] A. Ehn, T. Hurtig, P. Peterson, J. J. Zhu, A. Larsson, C. Fureby, J. Larfeldt, Z. Li, M. Aldén, “Setup for microwave stimulation of a turbulent low-swirl flame”, *J. Phys. D: Appl. Phys.* **49** 185601 (2016).

Setup for microwave stimulation of a turbulent low-swirl flame

Andreas Ehn[1*], Tomas Hurtig[2], Per Petersson[1], Jiajian Zhu[1], Anders Larsson[2], Christer Fureby[2], Jenny Larfeldt[3], Zhongshan Li[1] and Marcus Aldén[1].

[1]Combustion Physics, Lund University, PO Box 118, SE-221 00 Lund, Sweden

[2]Defence Security Systems Technology, The Swedish Defence Research Agency – FOI, SE 147 25 Tumba, Stockholm, Sweden

[3]Siemens Industrial Turbomachinery AB., SE-612 83 Finspång, Sweden

* Corresponding author: andreas.ehn@forbrf.lth.se

Key Words: plasma-assisted combustion, energetically enhanced combustion, turbulent flames, microwave enhancement, laser diagnostics, planar laser-induced fluorescence.

Abstract

An experimental setup for microwave stimulation of a turbulent flame is presented. A low-swirl flame is being exposed to continuous microwave irradiation inside an aluminum cavity. The cavity is designed with inlets for laser beams and a viewport for optical access. The aluminum cavity is operated as a resonator where the microwave mode pattern is matched to the position of the flame. Two metal meshes are working as endplates in the resonator, one at the bottom and the other at the top. The lower mesh is located right above the burner nozzle so that the low-swirl flame is able to freely propagate inside the cylinder cavity geometry whereas the upper metal mesh can be tuned to achieve good overlap between the microwave mode pattern and the flame volume. The flow is characterized for operating conditions without microwave irradiation using Particle Imaging Velocimetry (PIV). Microwave absorption is simultaneously monitored with experimental investigations of the flame in terms of exhaust gas temperature, flame chemiluminescence (CL) analysis as well as simultaneous planar laser-induced fluorescence (PLIF) measurements of formaldehyde (CH_2O) and hydroxyl radicals (OH). Results are presented for experiments conducted in two different regimes of microwave power. In the high-energy regime the microwave field is strong enough to cause a breakdown in the flame. The breakdown spark develops into a swirl-stabilized plasma due to the continuous microwave stimulation. In the low-energy regime, which is below plasma formation, the flame becomes larger and more stable and it moves upstream closer to the burner nozzle when microwaves are absorbed by the flame. As a result of a larger flame the exhaust

gas temperature, flame CL and OH PLIF signals are increased as microwave energy is absorbed by the flame.

Introduction

Research on plasma-assisted combustion (PAC) has attracted increasing interest the last decade due to the potential of combustion enhancement and control in power generation [1, 2]. PAC would serve as a valuable tool in damping the formation of combustion instabilities that are typically encountered in combustors with premixing of fuel and air for dry low emissions [3]. Implementing PAC would allow stable operation on even leaner gas mixtures than today, which would lower NO_x emissions. The downside of the lean operation and the inherent instabilities is twofold, since, a short term consequence is that mechanical instabilities cause severe hardware damage that may result in increasing cost. Further, the long term result is increased emissions with higher quantities of unburned hydrocarbons, which are known to be a far more effective greenhouse gas than carbon dioxide [4]. Low emission operation for cases of varying fuel quality as well as rapid changes in load could also be mitigated with PAC, i.e. better control of the combustion efficiency.

Most experimental investigations of PAC have been carried out on laminar flames. Investigations on laminar flames aim at providing experimental data that could be compared to chemical kinetics data from well-established low-dimensional modeling tools, such as CHEMKIN [5] and Cantera [6]. Detailed studies of such flames have proven to elucidate issues of e.g. laminar flame speed enhancement which can be used to distinguish the underlying physiochemical phenomena of

plasma-assisted combustion. However, combustion devices for large-scale power generation are based on turbulent combustion, where the combustion kinetics and fluid dynamics are intimately coupled. Therefore, experimental designs for electric stimulation of swirl stabilized turbulent flames needs to be investigated to understand the full effects of PAC in conditions that are adequate for power generation. This is of specific importance since the stimulation effects of plasmas depend on experimental conditions such as, for example, equivalence ratios and reduced electric field strengths [7]. Both these parameters vary significantly in turbulent flames where local variations in equivalence ratio and temperature alter the different conditions in combustion enhancement and thereby introduce new challenges on experimental designs.

There are a few ways to affect combustion with electricity such as for example high voltage discharge and microwave radiation. Compared to discharges there are certain advantages of using microwaves to study kinetic enhancement on combustion such as that microwaves are rapidly oscillating electric fields and thus do not cause combustion enhancement effects due to ionic wind and charged particle flux. For practical reasons microwave stimulation does not require electrodes in the vicinity of the flame which is favorable since electrodes have a certain lifetime in harsh environments that would result in degrading performance. In addition, microwave stimulation can be designed to have a volumetric effect which is ideal in studies of turbulent flames that indeed are volumetric objects without compromising with the flow symmetry.

Previous investigations that have been carried out at atmospheric conditions assert that continuous microwave stimulation of laminar flames have shown positive effects on the combustion [8-13]. Stockman et al. [8] report on a distinct increase in laminar flame speed in a methane/air flame by electric stimulation without forming a plasma discharge. By performing filtered Rayleigh scattering (FRS) they show a temperature increase just outside the flame zone of roughly 120 K. In two publications [9, 10], Shinohara et al. carried out laminar flame studies with electric field strengths below plasma formation. They also concluded on effects on laminar flame speed and found no sign of thermal heating from the spectral signatures of CH* and OH* flame chemiluminescence. Further, they reported an increase in flame chemiluminescence in the presence of microwaves and they measured the relaxation time of this additional signal intensity as they switched off their microwave system where time constants were found around 0.35-0.4 ms for their system. Rao et al. presented work where they defined the effects on the flame in different regimes depending on the amount of electric power that was added to the flame [13]. In regime 1, which is below plasma formation, both stability and laminar flame speed were enhanced which the authors attributed to thermal heating and in-situ reformation. As the microwave power was increased, a plasma was formed in the flame region. The plasma could be sustained without combustion and was therefore suggested to work as a flame holder in practical applications. A study by Zaidi et al. was carried out on a turbulent jet flame which was stabilized by a hydrogen pilot flame. Zaidi et al. demonstrated effects of microwaves

absorption on flame chemiluminescence data, with electric field strengths below breakdown threshold [12].

The design that is presented here aims at performing experimental studies of electrical stimulation of a freely propagating turbulent flame using microwave radiation. The setup allows investigations of flame chemiluminescence and laser based diagnostics with simultaneous monitoring of microwave absorption. Measurement results are presented for two different microwave power regimes, where the high power stimulation forms a swirl-stabilized plasma in the post-flame region. The plasma is sustained in the post-flame region by absorbing microwave energy resulting in increased exhaust-gas temperatures and strong plasma emission. In the low-power regime, below plasma formation, microwave stimulation shows a positive effect on the turbulent flame which indicates a kinetic enhancement of the turbulent flame speed.

Experimental setup

An overview of the experimental setup is shown in Figure 1a consisting of a microwave system including an alumina microwave cavity housing (Figure 1b), a low-swirl burner (Figure 1c) that operates with a co-flow and an optical measurement system.

Microwave system

The microwave system consists of an industrial magnetron (National Electronics GA15MP, 2.45 GHz) including a circulator and a load to absorb reflected power, sensors for incident and reflected power and a three stub tuner. The magnetron is capable of delivering up to 15 kW of microwave power into

a matched load. Electric-field sensors that are built into the circulator were used to monitor the incident and reflected microwave power. The damping of the signals was 63 dB between the sensors and the oscilloscope (LeCroy Wavemaster 8300). A maximum sampling rate of 20 G samples/s for two channels from the oscilloscope provides about eight sampling points per period for the microwave fields. Standard aluminum WR430 waveguides (with an inner width of 4.3”) were used to transfer the microwave radiation from the magnetron to the alumina resonator. The aluminum chamber (see Figure 1b) has two slits, located at opposite sides on the aluminum cavity, for input and output of laser beams. The height and width of the slit is 200 mm and 10 mm, respectively. The inlet slit is equipped with an alumina tube (length=50 mm and width=20 mm) that can be moved along the slit to provide laser measurements further downstream of the flame front. The inlet slit is sealed apart from the alumina tube preventing microwave leakage but still allow for laser access inside the aluminum resonator. A microwave sealed beam dump is mounted onto the output slit to minimize scattered laser light in the chamber. A visualization view port (150x50 mm^2) is located in-between the two slits for 90° detection of the laser induced signal. This view port is shielded by the use of two metallic meshes. Two metallic meshes are used to create a resonant cavity around the flame. The lower mesh is located just above (sub-mm) the burner nozzle which then defines zero on the Y-axis. The microwave mode pattern inside the resonator was experimentally investigated at the bottom of the chamber using temperature sensitive liquid crystal sheets (Edmund Optics). The mode pattern was mapped by a regular photography camera (Canon D650) through the view port and a projection

image with proper scaling was constructed through image analysis, displayed in Figure 1d. A capacitive sensor is mounted in the wall between the view port and the inlet slit for the laser (see the red cross in Figure 1b). The sensor was used to determine variations in local electric field strength during operation for different flame conditions.

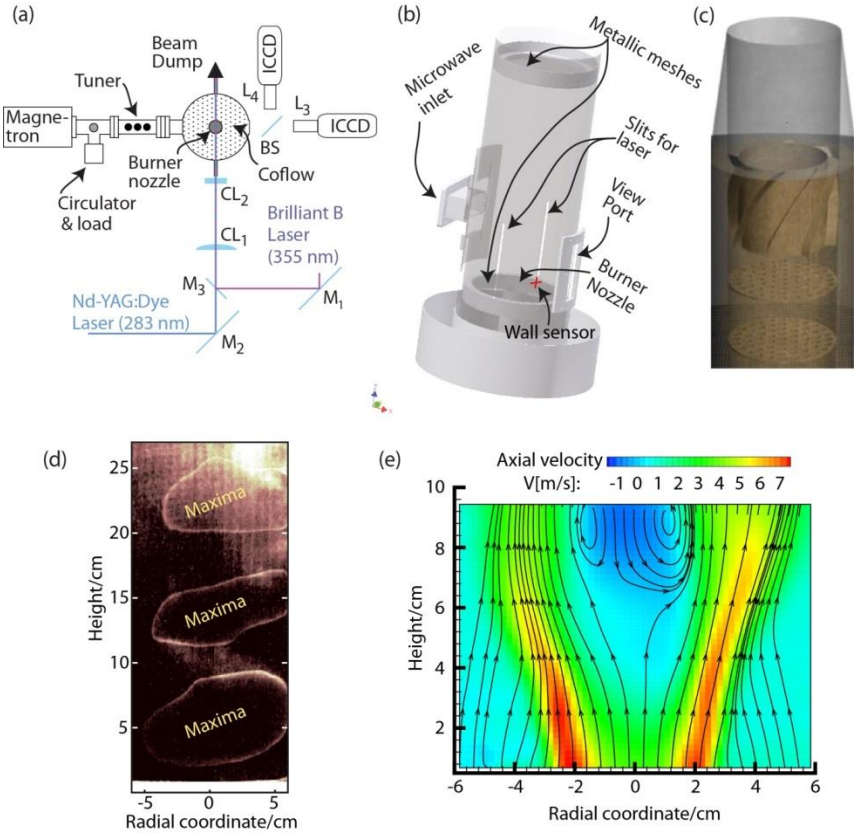

Figure 1 **(a)** Schematic overview of the experimental setup. Semitransparent images of **(b)** an aluminum microwave cavity resonator and **(c)** the low-swirl burner. **(d)** Mode pattern of the microwave electric field of a plane in the center inside the cavity without a flame present. **(e)** The 2D flow field (axial and radial velocity components) at the center plane above the burner, measured using PIV.

Low-swirl burner

The influence of microwave stimulation on a lean premixed lifted swirl stabilized flame was investigated using a low-swirl burner [14]. A semitransparent sketch of the low-swirl burner nozzle is displayed in Figure 1c. The low-swirl flow is created by an outer annular swirler, with eight swirl-vanes, in combination with an inner perforated plate [14]. About 60% by volume of the mixture pass through the swirler and 40% through the perforated plate [14]. After passing the swirler assembly premixed methane/air discharges through a 50 mm nozzle into the aluminum resonator cavity (300 mm in diameter) with an air co-flow of 0.4 m/s. The resulting outflow from the nozzle has an inner low velocity non-swirling region (-10 mm < r < 10 mm, where r is the radius) and an outer region with higher axial and tangential velocities [14-15]. The flow was investigated using Particle Imaging Velocimetry (PIV) showing that away from the nozzle the flow diverges causing the axial velocity in the center region to gradually decrease to create a low-speed region, see Figure 1e, where the freely propagating turbulent flame can be stabilized. It should be mentioned that the metallic mesh (2 x 2 mm^2 square holes and 64% transparency) just above the burner nozzle (see Figure 1a) modifies the flow field. By adding a mesh the radial transport from the outer high-speed regions towards the center is influenced, resulting in an increase in axial velocity. To assure well-controlled experimental conditions the set-up includes calibrated mass flow controllers for methane and air (Bronckhorst Hi-Tec, EL-Flow), and a flow meter for the co-flow (Fox, Thermal Instruments). All measurements were conducted in atmospheric conditions at room temperature with the flame operating with an equivalence ratio of 0.58 which corresponds to a theoretical flame power of 24 kW.

Optical arrangement

The optical arrangement for planar laser-induced fluorescence (PLIF) measurements is displayed in Figure 1a. Two laser systems were used to simultaneously study the spatial distribution of CH_2O and OH which are distributed in the preheat- and post-flame zone, respectively. Formaldehyde was probed by a frequency-tripled Brilliant B laser (Quantell) providing 355 nm laser pulses with a pulse duration of around 6 ns. Hydroxyl radicals were excited by using the $Q_1(8)$ transition in the $A^2\Sigma^+ \leftarrow X^2\Pi$ system using a Brilliant B pumped (532 nm) dye laser that was tuned to a wavelength around 283 nm. The lasers were overlapped using a dichroic mirror that transmitted 283 nm light. The laser beams were focused in the center of the low-swirl flame using a quartz cylinder lens (CL_1) with a focal length of 1000 mm. A negative quartz cylinder lens (CL_2), with a focal length of -40 mm, was used to expand the beams in the vertical direction to form a slightly diverging laser light sheet with an approximate height of 50 mm in the measurement volume. This type of diverging laser sheet was arranged in order to form a large-enough laser sheet through the microwave trap. A dichroic beam splitter (BS) with R>99.9% (λ_0 = 307 ± 20 nm) were used for separating the OH and CH_2O signals which were captured using different cameras. An ICCD camera (Istar 334T, Andor Technologies) was used to capture the formaldehyde fluorescence. The camera was equipped with a 50 mm/1.2 Nikon lens in combination with a pair of GG400 Schott filters (each 1 mm thick) to discriminate stray laser light. The OH signal was filtered by a UG 11 filter, mounted on a (f=100 mm) fused silica lens (Carl Zeiss F/4.0). The signal was captured by a CCD camera (Hamamatsu) that was operating with an

intensifier (Hamamatsu) that is optimized for UV. Spectroscopic measurements were performed using a spectrograph (Shamrock 750, Andor), equipped with a 1200 lp/mm grating, and an ICCD camera (Istar 334T, Andor Technologies). Flame emission for spectroscopic analysis was collected with a single lens configuration (f=200 mm) through the view port of the aluminum cavity. The horizontally oriented spectrograph slit was imaged (1:1) at height 55 mm downstream from the nozzle in the center of the flame. In addition, a high speed video camera (Fastcam SA-Z, Photron) was used to capture rapid events such as plasma formation.

Characterization of the reacting flow field (without microwaves) was carried out by use of 2D PIV, enabling two velocity components to be assessed in a plane through the center of the flow/flame region. A double cavity diode pumped kHz Nd:YLF laser (DualPower 1000-30, Dantec) with belonging light sheet optics was used as light source. The PIV data were acquired using a high-speed camera (SpeedSense 311, 1MP, 3250 fps). To eliminate background light and flame emission a narrowband 532 nm (+/-10 nm) interference filter was mounted on the (f=50 mm) camera lens. The PIV field-of-view had a height of ~100 mm to capture the overall characteristics of the flow field. Particles ($ZrSiO_4$), with an approximate diameter of 1 µm, were used to trace the methane/air flow and particles generated by smoke sticks were utilized for seeding the co-flow. The DynamicStudio software (v. 4.15) was used for the evaluation of the velocity fields measured by PIV.

Results

Typical flame chemiluminescence images are displayed in Figure 2 with and without microwave stimulation. The flame conditions in Figure 2 were identical apart from the microwave stimulation. The pictures reflect the impression from a direct visual observation of the flame. The flame becomes wider and brighter and it is stabilized at a lower position as the flame starts to absorb microwave radiation.

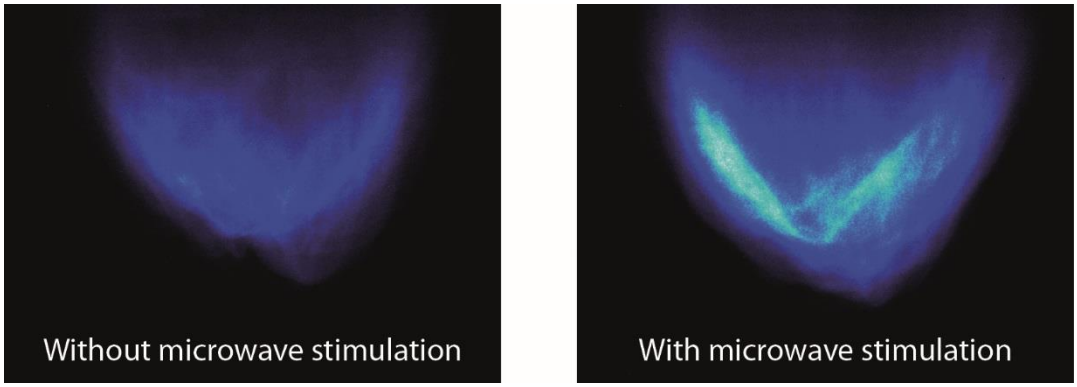

Figure 2 Typical single-shot pictures captured with an ICCD camera using 100 ms acquisition time. The flame clearly becomes wider, more luminescent and distinctly stabilized in a lower position in presence of microwaves.

The effect of microwave stimulation is directly linked to the amount of energy that is absorbed by the flame while correlation between input microwave energy and microwave stimulation is critically dependent on the overlap between the mode pattern and the flame. Hence, microwave absorption was continuously monitored during all experiments by sampling the incident and reflected microwave electric fields from the system. Typical waveforms of the incident and reflected electric fields of the microwaves are displayed in Figure 3a, where the difference in amplitude between the

two sinusoidal waveforms illustrates microwave absorption. Root-mean-square values of the waveforms were evaluated over 50 periods (~20 ns). Such rms-values were sampled and calculated with a rate of about 40 samples/s, as shown in Figure 3b. The rms-values of the electric fields were transformed into power by

$$P_i = \left[10^{\frac{\gamma}{20}} \cdot E_{RMS}\right]^2 \Big/ Z_0 \,, \qquad \text{(Eq. 1)}$$

where γ is the damping of the system in dB, E_{RMS} is the rms-value of the oscillating electric field and Z_0 is the input impedance. The damping of this system was 63 dB with input impedance of 50 Ω. The absorbed power, plotted as a black curve in Figure 3c, shows temporal variations in absorption inside the cavity, indicating that the microwave absorption occurred in non-continuous fashion. Variations in the electric field inside the resonator were monitored by a capacitive sensor, located at the surface of the aluminum cavity. Simultaneously monitoring of signals for the reflected microwave and the wall sensor show good correlation when the turbulent flame was stimulated by microwave emission (Figure 4a). The mode pattern was stable without a flame present in the resonator to absorb microwave energy (Figure 4b) and virtually no absorption occurs. In addition, the local field strength at the wall sensor was significantly affected by changing the equivalence ratio of the flame. Altogether, these investigations indicate that the most significant variation in microwave absorption is due to the flame itself which is an unstable turbulent hot object with high amounts of charged species compared to the surrounding air. Further, the flame volume and the charge particle

distribution increase as a flame absorbs microwave power which affects the microwave mode pattern.

A thermocouple, located just above the center of the upper metallic mesh (at height 55 cm), was used to monitor the gas temperature of the exhaust gas. An increase in the exhaust gas temperature was noticed as the flame started absorbing microwave energy. The increase of the exhaust gas temperature correlated well with the amount of energy that was absorbed by the flame. The reflected microwave power as well as the exhaust gas temperature was used as an indicator of good microwave coupling when the stub tuners and the resonator geometry was tuned to achieve high microwave stimulation.

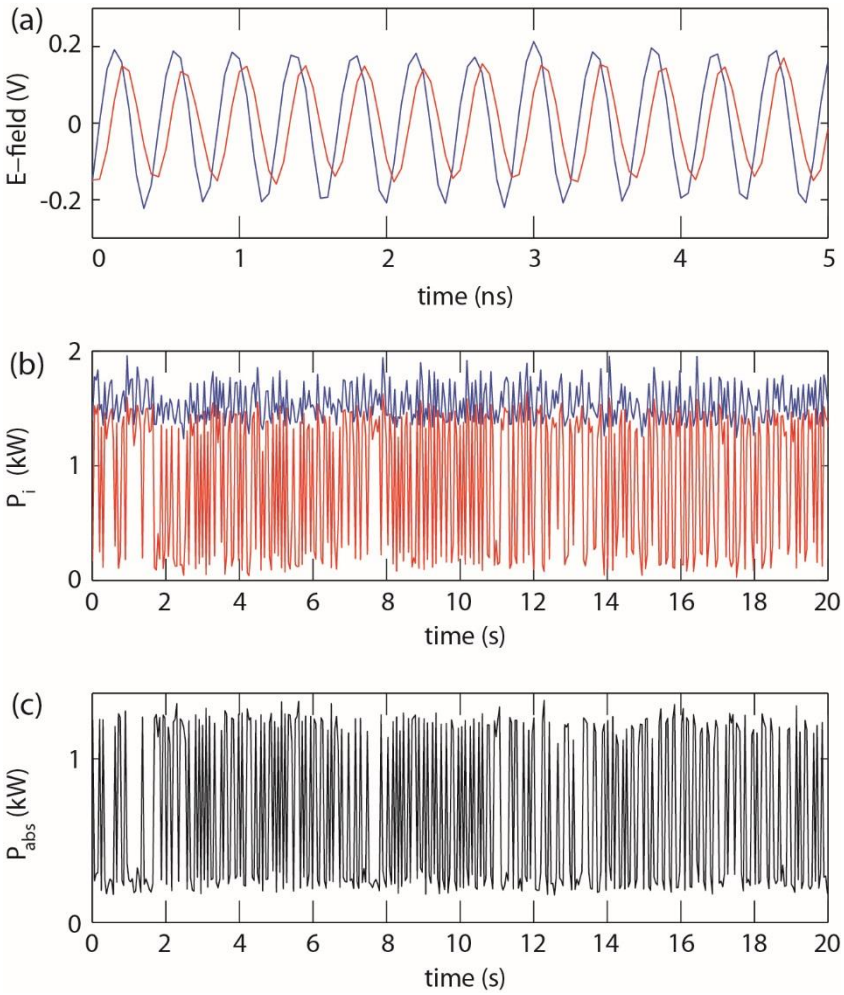

Figure 3 **(a)** Oscillating electric field strength of the incident (blue) and reflected (red) microwave radiation with a frequency of 2.45 GHz (which corresponds to a period around 0.4 ns). The difference in amplitude is caused by absorption of the flame. **(b)** Continuously trended rms-values of the incident (blue) and reflected (red) microwave power. **(c)** Differential absorbed microwave power.

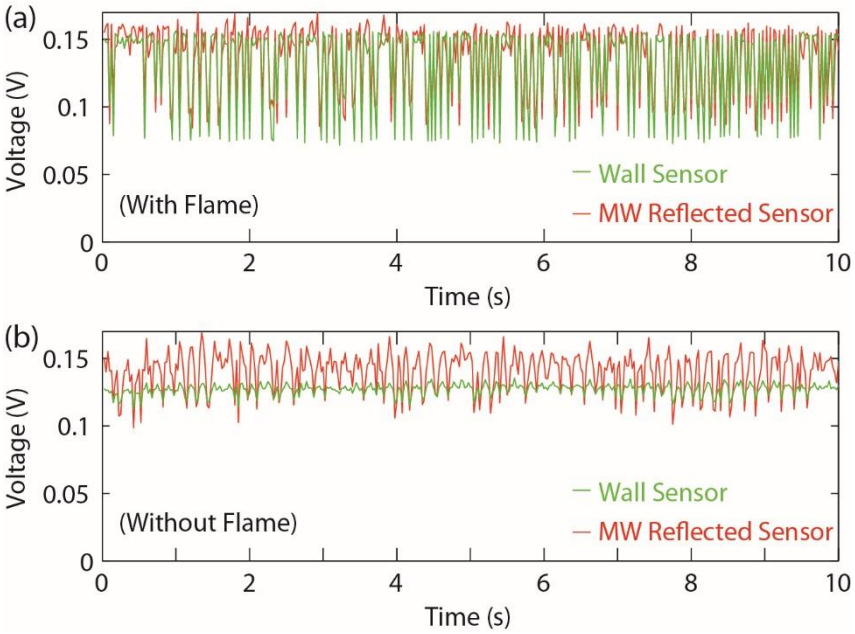

Figure 4 Sensor signal of the reflected microwave (red) along with the signal from the capacitive sensor that is located close to the wall (green). Measurements were conducted with **(a)** and without **(b)** a flame present in the cavity.

An increase in the incident microwave power increased the electric field strength inside the cavity for an accurately tuned resonator. High enough electric field strengths caused breakdown in the flame if the cavity modes were properly tuned. Such an event was captured with a high-speed camera and four images are displayed in Figure 5. Breakdown occurred in the vicinity of the flame front since the reduced electric field scales linearly with temperature (at constant pressure) and because the number of free electrons is higher at the flame front [16]. The breakdown occurred in the flame when a strong microwave electric field were employed, see Figure 5 at t = 0. In addition, a strong electric field could cause the free charges in the initial small plasma to accelerate and create a charge particle avalanche. The avalanche enables the plasma to grow as displayed in Figure 5 at times t =

12.1 and 24.2 ms. After further microwave absorption a fully developed flow-stabilized plasma anchored in the product region of the flame which was seen after about 36 ms. Note that this is line-of-sight data and therefore the position of the breakdown in the image is concomitant with an unresolved three dimensional effect. Hence, the absolute height where the breakdown occurred cannot be related to a vertical position in these images. Such tests were used to achieve good alignment between the flame and the mode pattern of the microwave at the measurement condition of interest. In cases where this alignment is off, breakdown could occur close to sharp metal edges inside the resonator due to local field enhancement at higher microwave input powers.

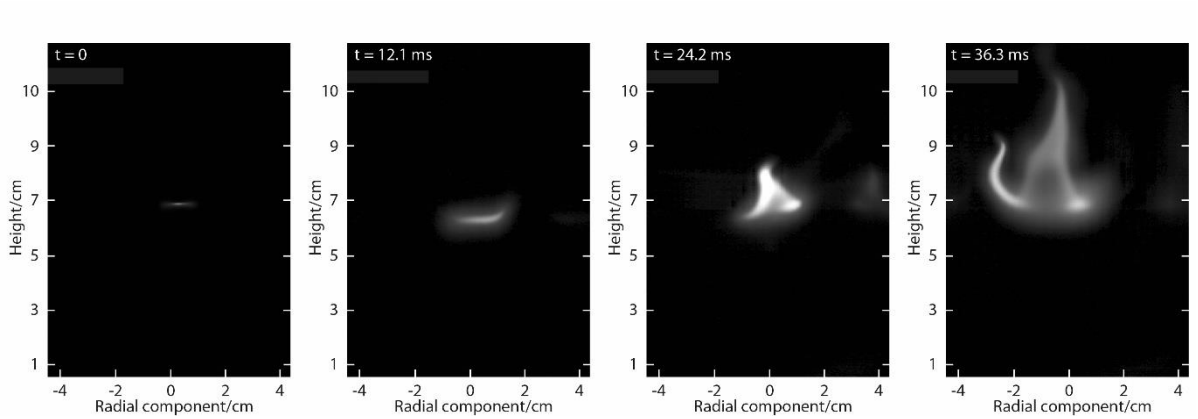

Figure 5 An image sequence recorded by a high-speed camera where the microwaves cause a breakdown in the flame. The initial small breakdown volume absorbs microwave radiation and develops to a swirl-stabilized plasma volume located in the post-flame region.

Simultaneous PLIF measurements of OH and CH_2O were carried out. Typical PLIF images of CH_2O and OH are displayed in the left panel in Figure 6 when the flame is stimulated by microwaves. The red and green signals correspond to CH_2O and OH, respectively. The flame front in the lower central part of the flame is continuous and flamelet-like, showing a well-defined thin preheat region where

formaldehyde appears. Formaldehyde is consumed in the steep temperature gradient in the reaction zone whereas OH consumption is reduced in the post-flame region resulting in a supersaturated region of OH. Further away from the flame front, in the product region, OH concentrations decreases mainly due to formation of water.

Measurements were also conducted when a fully developed plasma interacts with the flame. The presence of such a plasma creates an increased thermal expansion that influences the flame volume and moves the flame front closer to the burner nozzle. The OH-signal is clearly enhanced whereas the formaldehyde seems unaffected by the plasma. The preheat zone appears closer to the plasma when the equivalence ratio is decreased and the flame can actually be removed leaving the swirl stabilized plasma freely propagating in the swirling flow. The exhaust gas temperature substantially increased when such a plasma was formed and spectroscopic analysis of the plasma emission shows large signals of OH and also spectral features of NO. Both images in Figure 6 show PLIF signals from OH and CH_2O of a microwave stimulated low-swirl flame. The microwave input energy is ~2.4 kW in both conditions, which is right at the limit of plasma formation in these conditions. The emission from the plasma is extremely intense so that the gated detection is not sufficient to suppress the plasma emission which is displayed in the right panel in Figure 6.

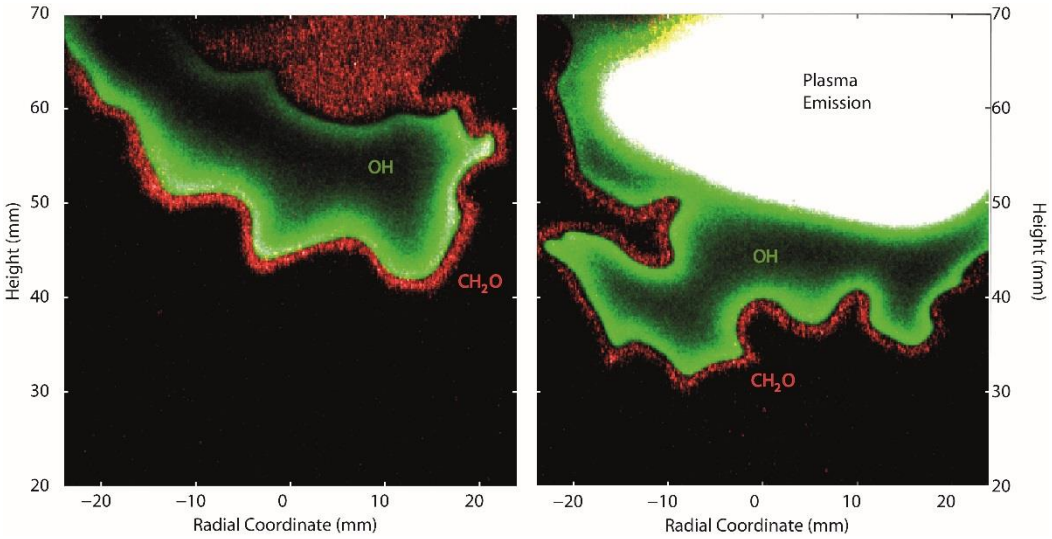

Figure 6 Results from simultaneous PLIF imaging of OH (green) and CH_2O (red) of the low-swirl flame. The flame is stimulated by microwaves in both experimental conditions with equal amount of input microwave power to the resonator (~2.4 kW). A plasma has developed in the flame to the right whereas no plasma is present in the measurement data to the left.

Spectroscopy and imaging were performed on the excited OH flame chemiluminescence as the flame was stimulated by microwaves at lower microwave input powers. The amount of energy absorbed by the flame shows no effect on the shape of the OH emission spectra, which is in line with what was reported by Shinohara et al. [9], for a laminar flame. Averaged imaging data of OH* flame emission, displayed in Figure 7, clearly shows an increase in flame chemiluminescence with 1.1 kW microwave absorption without plasma formation. Imaging of flame chemiluminescence collects line-of-sight emission and therefore this signal reflects the entire flame volume. The increased flame volume is more pronounced when the flame chemiluminescence data in Figure 7 is presented as a ratio image. The image ratio, shown in Figure 8, is formed by having the microwave stimulated data in the

denominator and the reference flame in the numerator, resulting in low ratios in locations where the flame chemiluminescence increase with microwave stimulation. A signal threshold was used to create the ratio image for the flame chemiluminescence data so as to reduce background noise in regions without contributing flame chemiluminescence. The ratio image in Figure 8 clearly shows a relatively higher increase in flame chemiluminescence at the edges and at the bottom of the flame kernel. These observations clearly indicate that the flame volume is increased and that it is stabilized closer to the burner nozzle when the flame is absorbing microwave radiation.

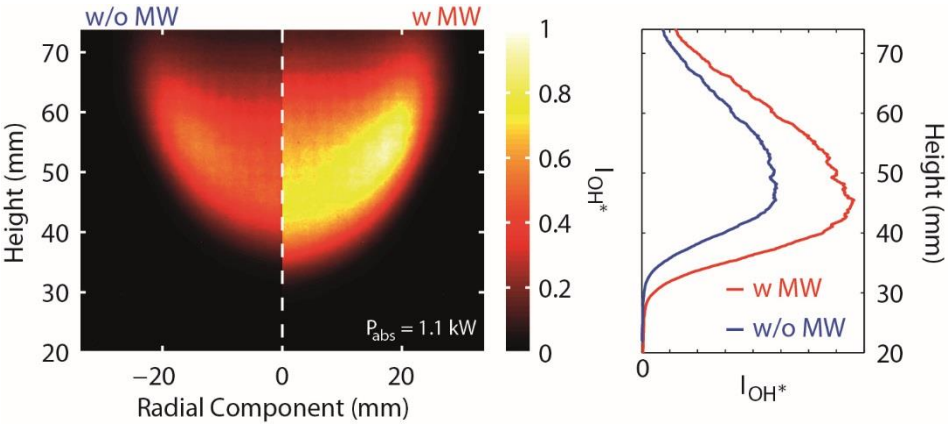

Figure 7 Flame chemiluminescence from excited OH. The left hand side of the image shows the flame without microwave stimulation whereas the right part of the image shows the flame chemiluminescence of a flame that absorbs around 1.1 kW of microwave power. The microwave input power was approximately 2.15 kW. The graph to the right shows cross-section data (around the dashed white line in the left panel) in the center of the two flames.

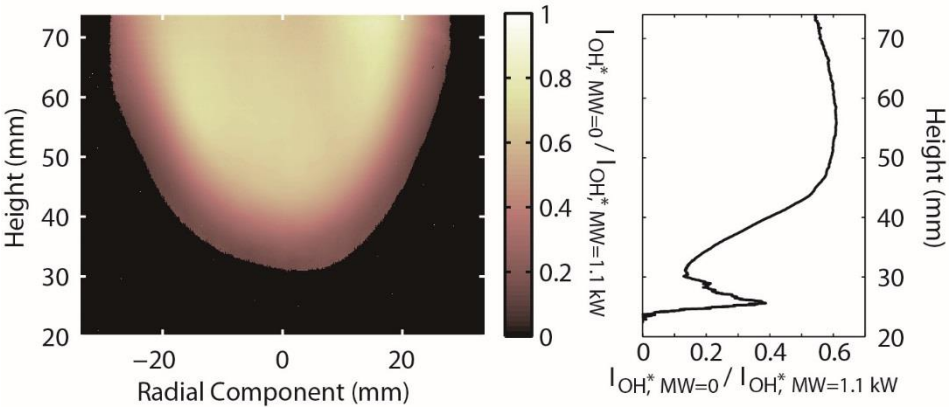

Figure 8 The image to the left shows a spatially distributed ratio of flame chemiluminescence from the two flames that are imaged in Figure 7. The graph to the right shows a cross section of the center of the ratio image. The peak located just below 30 mm from the nozzle is a result of noise. This noise has been removed in the ratio image by setting a threshold value of around 1% of the maximum signal for the image in the numerator.

Discussion

The microwave absorption by the flame could be estimated by measuring the incident and reflected microwave power. However, the absolute amount of energy that is absorbed by a large turbulent flame is not straight forward to quantify. In addition, the energy that might be absorbed by another sink than the flame is also hard to estimate since the microwave mode pattern is changed when the flame is turned off. Then again, most of the energy is reflected when the system is operating in absence of the flame and therefore a second sink term is neglected when the amount of absorbed energy is estimated in this current investigation. As mentioned in previous publications, e.g. Zaidi et al. [12], where a flame is inserted into a resonator, system tuning is critical for optimization of microwave absorption by the flame. This current investigation involves a fairly large swirl-stabilized turbulent flame which obviously is dynamic in its nature. The large-scale turbulent flame can affect

the conditions in the cavity during operation and therefore the average energy absorption of the flame is determined for all measurements that were conducted. The resonator used by Zaidi et al. is, to the knowledge of the authors, a bit different since the resonator that is used in this current study is heavily over-moded in all three directions while that used by Zaidi et al. is only over-moded in one direction. Technically, this means that there are several possible Eigen-mode solutions that are very close to each other, making the mode pattern easily affected and less stable. However, a large resonator is needed for a large-scale turbulent flame and since the wavelength associated with the 2.45 GHz frequency used in these experiments is about 12 cm it is significantly smaller than all geometrical dimensions of the resonator, hence the resonator will be over-moded.

Coupling between electromagnetic radiation and the flame has been discussed in a number of experimental investigations for laminar flames and continuous microwaves. Zaidi et al. presented absorption values below 1% in [17] and of about 10 % in [12] for laminar flames. Peaks of rather high absorption of microwave power by the flame are reported in the present study even though the absorption was somewhat unstable, indicating that the size of the flame affects the amount of absorbed microwave energy. The propagation of an electromagnetic wave in a linear and isotropic medium can be expressed by the Helmholz equation,

$$\nabla^2 \boldsymbol{E} - \gamma^2 \boldsymbol{E} = 0, \qquad \text{(Eq. 2)}$$

where $\boldsymbol{E}$ is the electric field and γ is the complex propagation constant, see for example [18]

$$\gamma = \alpha + j\beta = j\omega\sqrt{\epsilon_0\mu_0}\left(1 + \frac{\sigma}{j\omega\epsilon_0}\right)^{\frac{1}{2}}. \quad \text{(Eq. 3)}$$

Here ϵ_0 and μ_0 are the permittivity and permeability of vacuum and σ is the conductivity of the medium that can be expressed as

$$\sigma = \frac{n_e e^2}{m_e v_c}, \quad \text{(Eq. 4)}$$

where e, n_e m_e and v_c are the electron charge, density, mass and collision frequency. The real part of Eq 3, α, describes the attenuation of the wave in the medium and the imaginary part describes the phase shift that occurs when the wave travels in the medium. The inverse of the attenuation constant for a good conductor is called the 'skin depth' and describes how high frequency signals rapidly attenuate when propagating in a good conductor. A flame, however, is not a good conductor since the electron density and collisional frequency is rather low compared to a good conductor, such as a metal. In a flame, the collision frequency, v_c, will be on the order of 10^{12} Hz at atmospheric pressure conditions according to calculations using the software Bolsig+ [19]. The background electron density in a propane/air flame was measured by McLatchy to about 3.5 * 10^{17} m^{-3} [16]. Some work indicate slightly lower electron densities in a methane/air flame [20-22], but the lower values may be due to a less exact experiment than what was performed by McLatchy. Using the above values for n_e and v_c and *f*=2.45 GHz, σ is found to be 0.025 S/m, resulting in $\alpha \approx 4.6$ [Np/m], giving a penetration depth of $1/\alpha \approx 0.22$. I.e. the amplitude of the electric field is attenuated by 1/e at a distance of 22 cm into a medium with v_c and n_e as given above. The value for electron density

used here is not valid for the entire flame since the main electron production occurs in a limited region through the chemiionization process: $CH + O \rightarrow HCO^+ + e^-$. Altogether, the penetration depth explains, at least in part, the modest microwave absorption of smaller flames [12, 16] contrary to the stronger absorption that is achieved with a larger flame which momentarily can go up above 50%. Miles and coworkers have shown an increase in absorption to about 60% when using pulsed microwaves with high peak powers [23]. The high peak power in those experiments gives rise to much higher electron density and temperature than in the experiments reported here and this is most probably the explanation for the high microwave absorption reported. In summary, pulsed microwave stimulation of larger flames should yield rather high absorption, making microwave stimulation an attractive solution for plasma-assisted combustion under technically relevant conditions.

Enforcing plasma ignition in the flame serves an excellent instrument of optimizing the spatial overlap between the flame and the microwave mode patterns. Such tests can be performed at the measurement conditions of interest and this is crucial since the flame affects the mode pattern. However, the fully developed plasma that stabilizes in the product region seems to mostly affect the flame front by gas heating since it is located downstream of the flame front with which the plasma has minor interaction. This should, in principle, be the case for continuously fed hot plasmas for combustion enhancement because the flame is adjusting to the gas heating plasma. Hence, the flame front cannot overlap with the plasma if the gas is hot enough to ignite the combustible gas mixture.

Such issues can obviously be avoided by using a pulsed high voltage source if the flame dynamic is much slower than pulsed discharges or microwave pulses. In addition, gas heating is minimized by using short pulses [23], which have been investigated by Miles and coworkers [24]. A somewhat alternative approach was used by Rao et al. [13] who achieved strong electric fields by utilizing local field enhancement. On one hand, local field enhancement occurs close to sharp metal edges which then preclude electric field stimulation of freely propagating flames. On the other hand, as is stressed by the authors, this design is more relevant for flame stabilization and combustion control and the strongest field enhancement is found fairly far upstream in the combustible gas mixture flow.

Spectral signatures of flame chemiluminescence of OH* and CH* were observed to have the same shape with and without microwave stimulation (as long as no breakdown occurs). The unaffected shapes of the spectra were also reported by Shinohara et al. [9] who interpret this as indications that the local temperature was unaffected by microwave stimulation. Assessing flame temperatures from flame chemiluminescence is a rather rough approach since it is based on line-of-sight information that will be affected by self-absorption in the flame. Spectral studies of flame chemiluminescence from CH*, however, have been proposed for estimation of flame temperatures in e.g. Gaydon [25] even though it is not obvious what kind of temperature information CH* emission actually displays. More rigorous attempts to determine flame temperatures were carried out by Stockman et al. using filtered Rayleigh scattering (FRS) [8]. They reveal a temperature increase with microwave stimulation of around 125 K just out of the flame front of a lifted laminar methane/air flame where the

temperature was around 2000 K. This is actually close to the position where CH* is formed [26] indicating that there probably is a moderate increase in local temperature even though the shape of the emission spectra seems unaffected from microwave stimulation. The substantial increase in exhaust-gas temperature is evidently a result from microwave stimulation which is seen to increase the chemical activity of the flame.

The local equivalence ratio is highest at the leading edge of the low-swirl flame whereas additional air is being entrained into the fuel stream along the flame brush. This stratification results in a reduction of the local equivalence ratio with height at the edges of the flame. As microwave stimulation can increase the chemical activity the effect of the stratification can be reduced making the flame broader. In addition, an increased flame speed also affects the mean position of the flame base and hence, the flame is stabilized closer to the nozzle when microwave stimulation is established (see Figure 1e). This increased flame activity results in a larger flame volume and a more stable flame, which is evident from Figure 7 and Figure 8.

Concluding remarks

A setup for conducting investigations of microwave stimulated combustion on turbulent large scale swirl-stabilized flames is demonstrated and employed. The flame is kept inside a microwave aluminum cavity with the microwave mode pattern optimized to overlap with the flame position. Optical measurements were conducted with simultaneous monitoring of the incident and reflected microwave fields, which is utilized to estimate the microwave absorption by the flame. The dynamic

nature of the flame is reflected in temporal variation in microwave absorption by the flame where high peak values are noticed for the absorption (above 50%).

Tests were also performed with higher electric fields that causes breakdown in the flame. These tests show that a swirl-stabilized plasma can be generated and supported by microwave energy in the product region of the flame. The hot plasma pushes the flame closer to the nozzle due to thermal expansion and the gas heating is significant enough for the plasma and the flame front never to directly interact. The two pools of radicals, from the plasma and the reaction zone, never overlap since the temperature in the vicinity of the plasma is hot enough to ignite the flame from the post-flame side.

Clear effects of microwave stimulation on the large turbulent flame characteristics are summarized as: (1) the flame stabilizes closer to the burner nozzle, (2) the flame volume is increased and (3) the exhaust gas temperature is increased. Altogether, these are all effects that are of utmost interest in combustion enhancement and control.

Acknowledgements

This work was financially supported by the Swedish Energy Agency as well as Knut and Alice Wallenberg Foundation as well as ERC through the project TUCLA. OH-PLIF measurements were conducted with assistance from Dantec Dynamics. Also, Jiajian Zhu would like to thank China Scholarship Council for financial support.

References

1. A. Starikovskiy, N. Aleksandrov, Plasma-assisted ignition and combustion, Prog. Energy Combust. Sci. 39 (2013) 61.
2. Y. Ju, W. Sun, " Plasma assisted combustion: Dynamics and chemistry", Prog. Energy Combust. Sci., 48 (2015), pp. 21–83.
3. K. R. McManus, T. Poinsot and S. M. Candel, "A review of active control of combustion instabilities", Prog. Energy Combust. Sci. 1993, Vol. 19, pp. 1-29.
4. H. Rodhe, "A Comparison of the Contribution of Various Gases to the Greenhouse Effect", Science, New Series, Vol. 248, No. 4960, pp. 1217-1219
5. R.J. Kee, F.M. Rupley, J.A. Miller, M.E. Coltrin, J.F. Grcar, E. Meeks, H.K. Moffat, A.E. Lutz, G. Dixon-Lewis, M.D. Smooke, J. Warnatz, G.H. Evans, R.S. Larson, R.E. Mitchell, L.R. Petzold, W.C. Reynolds, M. Caracotsios, W.E. Stewart, P. Glarborg, C. Wang, C.L. McLellan, O. Adigun, W.G. Houf, C.P. Chou, S.F. Miller, P. Ho, P.D. Young, D.J. Young, D.W. Hodgson, M.V. Petrova, K.V. Puduppakkam, CHEMKIN Release 4.1, Reaction Design, San Diego, CA, 2006.
6. Goodwin, D.G., 2003. An open‐source, extensible software suite for CVD process simulation. In Proceedings of CVD XVI and EuroCVD Fourteen, M Allendorf, F Maury, and F Teyssandier (Eds.), Electrochemical Society, 155-162.
7. W. Rao, "Laser Diagnostics of Plasma Assisted Combustion", Dissertation thesis from Michigan State University 2010.

8. E.S. Stockman, S.H. Zaidi, R.B. Miles, C.D. Carter, M.D. Ryan, “Measurements of combustion properties in a microwave enhanced flame”, Combustion and Flame 156 (2009) 1453–1461.

9. K. Shinohara, N. Takada, and K. Sasaki, "Enhancement of burning velocity in premixed burner flame by irradiating microwave power", J. Phys. D: Appl. Phys. **42** (2009) 182008.

10. Koichi Sasaki and Koji Shinohara, “Transition from equilibrium to nonequilibrium combustion of premixed burner flame by microwave irradiation”, J. Phys. D: Appl. Phys. **45** (2012) 455202.

11. K. Sasaki, K. Shinohara and N. Takada, “Enhancement of burning velocity in premixed burner flame due to electron heating by microwave irradiation”, 49th AIAA Aerospace Sciences Meeting including the New Horizons Forum and Aerospace Exposition 4 - 7 January 2011, Orlando, Florida

12. S.H. Zaidi, E. Stockman, X. Qin, Z. Zhao, S. Nacheret, Y. Ju, R.B. Miles, D.J. Sullivan, J.F. Kline, “Measurements of Hydrocarbon Flame Speed Enhancement in High-Q Microwave Cavity”, 44th AIAA Aerospace Sciences Meeting and Exhibit 9-12 January 2006, Reno, Nevada, US.

13. X. Rao a, K. Hemawan, I. Wichman, C. Carter, T. Grotjohn, J. Asmussen, T. Lee, “Combustion dynamics for energetically enhanced flames using direct microwave energy coupling”, Proceedings of the Combustion Institute 33 (2011) 3233–3240.

14. P. Petersson, J. Olofsson, C. Brackman, H. Seyfried, J. Zetterberg, M. Richter, M. Alden, M.A. Linne, R.K. Cheng, A. Nauert, D. Geyer, and A. Dreizler, *Simultaneous PIV/OH-PLIF, Rayleigh*

thermometry/OH-PLIF and stereo PIV measurements in a low-swirl-flame. Applied Optics, 2007. **46**(19): p. 3928-3936.

15. K.J. Nogenmyr, C. Fureby, X.S. Bai, R. Petersson, R. Collin, and M. Linne, *Large eddy simulation and laser diagnostic studies on a low swirl stratified premixed flame.* Combustion and Flame, 2009. **156**(1): p. 25-36.
16. C.S. MacLatchy, "Langmuir Probe Measurements of Ion Density in an Atmspheric Pressure Air-Propane Flame", Combustion and Flame, **36**, (1979) 171-178.
17. S.H. Zaidi, S. Macheret, L. Vasilyak, R.B. Miles, Y. Ju, D.J. Sullivan, "Increased speed of Premixed laminar flames in a microwave resonator", 35th AIAA Plasma dynamicsand laser conference, Portland, 28 Juni 1 Juli (2004).
18. D.K. Cheng, "Field and Wave Electromagnetics", Addison-Wesley Publishing, November 1992, ISBN 0-201-12819-5
19. G. J. M. Hagelaar and L. C. Pitchford," Solving the Boltzmann equation to obtain electron transport coefficients and rate coefficients for fluid models", Plasma Sources Sci. Techn. 14 (2005) 722-733.
20. G. Wortberg " Ion-concentration measurements in a flat flame at atmospheric pressure", Tenth Symposium on Combustion, The Combustion Institute, Pittsburgh, 1965, p 651
21. H. F. Calcote, "Ion and electron profiles in flames", Ninth Symposium on Combustion, The Combustion Institute, Pittsburgh, 1963, p 622

22. J. Peeters, Oxidation and Combustion Reviews, Elsevier, Amsterdam, 1969, Vol. 4, p 93

23. I V Adamovich, I Choi, N Jiang, J-H Kim, S Keshav, W R Lempert, E Mintusov, M Nishihara, M Samimy and M Udd, “Plasma assisted ignition and high-speed flow control: non-thermal and thermal effects”, Plasma Sources Sci. Technol. 18 (2009) 034018 (13pp).

24. J. B. Michael, T. L. Chng, R. B. Miles, “Sustained propagation of ultra-lean methane/air flames with pulsed microwave energy deposition”, Combustion and Flame 160, (2013) 796-807.

25. A. G. Gaydon, “The Spectroscopy of Flames”, 2nd Edition, Chapman and Hall, London 1974.

26. J. Kojima, Y. Ikeda, T. Nakajima, ”Basic aspects of OH(A), CH(A), and C2(d) chemiluminescence in the reaction zone of laminar methane–air premixed flames”, Combustion and Flame 140 (2005) 34-45.